

Vector-Neutrino Interaction in a Screening Framework, and Neutrino Oscillation

H. Yazdani Ahmadabadi* and H. Mohseni Sadjadi†

Department of Physics, University of Tehran,
P. O. B. 14395-547, Tehran 14399-55961, Iran

September 28, 2022

Abstract

A vector field is assumed to be conformally coupled to the matter components through a screening mechanism. The matter density implicitly affects the neutrino flavor transitions through the vector field. We study the neutrino-vector field interaction in the presence of a finite-size matter density like the Sun and compute the discrepancy in the total flux of solar electron-neutrinos. Considering existing neutrino flavor conversion data, we find that for the non-standard vector-neutrino interactions, significant matter effects might be possible.

1 Introduction

The phenomenon of neutrino oscillations has been established as the most plausible mechanism behind neutrino flavor transitions [1–3], while an additional sub-leading effect caused by neutrino decay has been studied more recently in a two-generation model in [4, 5]. Originating from a damping factor, the net effect of the decay is depletion in the total neutrino flux and consequently on the neutrino transition probabilities on the Earth. The physics beyond the standard model (BSM) may appear as unknown couplings involving neutrinos, usually referred to as non-standard interactions (NSIs) [6–8]. Such interactions, pioneered by [9], may modify the neutrino evolution inside matter through an effective Wolfenstein potential induced by the scalar or vector field interactions with neutrino/matter components [8, 10].

Since the mass scale of neutrinos is similar to the dark energy scale, neutrino physics is often considered an exceptional window to cosmology [11–16]. Among the various scalar-tensor dark energy models for explaining the cosmic acceleration of the Universe, some models might be described by a matter-scalar conformal coupling classified as chameleon [17–20] and symmetron models [21–27]. A general feature of these models to explain the nature of dark energy is that they modify general relativity at cosmological scales but recover that at small scales. This type of coupling is also defined so that when the massive neutrinos became non-relativistic, the Universe’s acceleration starts by activating the quintessence [28–30].

In [4, 5, 31–33], the conformal coupling is studied as an interaction between the quintessence and neutrinos, which affects the neutrino flux and flavor transition and induces an MSW-like effect.

Neutrinos can couple not only to scalar fields but also to vector fields [8, 10]. Like the conventional scalar NSI, the vector-type interaction contributes as a correction to either the neutrino mass or the matter Wolfenstein potential.

The screening model may also be extended to vector-tensor models, where the coupling of the vector field to matter makes it vanish in dense regions [26]. Considering the coupling to the neutrinos as an interaction, allowing energy exchange with the vector boson, one could investigate the influence of this interaction on neutrino oscillation.

We present a study of the effective potential induced by a light vector mediator in the context of the screening vector-tensor model. We consider the coupling as an interaction and the dark vector boson, and

*hossein.yazdani@ut.ac.ir

†mohsenisad@ut.ac.ir

we compute the Wolfenstein potential for a spherically symmetric density profile like the Sun. We study the new mass and energy dependencies on the coupling constants. Diagonalizing the neutrino Hamiltonian may introduce the effective matter potential to determine the mass and mixing parameters.

This paper is organized as follows. In section 2, we review and discuss a vector screening mechanism inside and outside the body in which the vector field hides on small scales while producing relevant cosmological signatures. The solution to the Dirac equation in the conformally flat spacetime has been given in section 3, where the mass and energy of neutrinos obtained new forms. The vector NSI with matter components, including neutrinos and its phenomenological consequences, are explored in section 4. This section will also discuss the possibility of neutrino decay and depletion in the total probability. Furthermore, the vector-matter NSI might impact the neutrino Hamiltonian, resulting in the effective mass and mixing parameters. Solar neutrinos can be used to probe for physics BSM that affects neutrino interactions with the vector boson. Therefore, we restrict our model of neutrino flavor conversion plus decay, including the recent Borexino [34] and SNO+Super-Kamiokande [35] data in section 5.

Throughout the paper, we use units $\hbar = c = 1$ and metric signature $(+, -, -, -)$.

2 Vector screening model

In this model, in which screening occurs due to a spontaneous symmetry breaking, the conformal factor depends on the norm of the vector field A_μ . The most action for the massive vector field is

$$S = \int d^4x \sqrt{-g} \left[\frac{M_p^2}{2} \mathcal{R} - \frac{1}{4} F_{\mu\nu} F^{\mu\nu} - \frac{1}{2} (\partial_\mu A^\mu)^2 - \frac{1}{2} m_A^2 A^2 \right] - \int d^4x \mathcal{L}_m [\tilde{g}_{\mu\nu}, \Psi], \quad (1)$$

where \mathcal{R} is the Ricci scalar with respect to the metric $g_{\mu\nu}$, $F_{\mu\nu} = \partial_\mu A_\nu - \partial_\nu A_\mu$ is the vector field strength tensor. \mathcal{L}_m is the Lagrangian of the massive matter components. $\tilde{g}_{\mu\nu}$ is related to the metric $g_{\mu\nu}$ via

$$\tilde{g}_{\mu\nu} = B^2(A^2) g_{\mu\nu}. \quad (2)$$

Here $A^2 = g^{\mu\nu} A_\mu A_\nu$ and the conformal coupling function with strength β is given by an exponential factor $B(A^2) = \exp(\beta A^2/M_p^2)$. The coupling B induces an interaction between the matter and the vector boson.

By varying the action (1), the evolution equation for the massive vector field is given by

$$\square A_\mu = \left[m_A^2 - \frac{2\beta\rho}{M_p^2} e^{\frac{\beta A^2}{M_p^2}} \right] A_\mu, \quad (3)$$

where we have used the rescaled density $\rho \equiv e^{3\beta A^2/M_p^2} \tilde{\rho}$ for the pressureless matter. In the case of a conformal coupling depending on a scalar field ϕ , one finds the energy-momentum tensor $T_{\mu\nu} = B^2(\phi) \tilde{T}_{\mu\nu}$ [17], whereas, in the case of a conformal factor depending on the vector field, we obtain [26]

$$T_{\mu\nu} = B^2(A^2) \left[\tilde{T}_{\mu\nu} - 2B(A^2)B'(A^2) \tilde{T} A_\mu A_\nu \right], \quad (4)$$

where the prime denotes differentiation with respect to A^2 . In such a case, the additional term appears because the argument of the conformal factor $B(g^{\mu\nu} A_\mu A_\nu)$ depends on the metric. This term is necessary only when the matter component is relevant and can be the source of large-scale anisotropic stress [26]. Despite the anisotropy of the oscillations, the averaged energy-momentum tensor is isotropic [36].

The field equations (3) can be considered a set of four scalar fields. Their effective interaction couples all four components. The medium particles can mostly be considered non-relativistic, hence $\tilde{\Psi} = n_\Psi$ and $\tilde{\Psi} \gamma^\mu \Psi = n_\Psi (1, 0, 0, 0)$ [10]. Since the number density of solar neutrinos is much smaller than that of electrons or nucleons, the source of the vector field A_μ is mainly the medium particle and not the neutrinos [10]. Thus, we can suppose that the spatial components of A_μ vanish, i.e., $A_\mu = (A_0, 0, 0, 0)$. Furthermore, A_0 has no time dependence, i.e., $\partial_t A_0 = 0$, since the medium particles are at rest. Therefore, the equations of motion can be approximated by

$$\square A_0 = \left[m_A^2 - \frac{2\beta\rho(r)}{M_p^2} e^{\frac{\beta(A_0)^2}{M_p^2}} \right] A_0. \quad (5)$$

Now, we can define the following effective potential for the temporal component:

$$V_{\text{eff.}} = -\frac{1}{2}m_A^2(A_0)^2 + \rho(r)e^{\frac{\beta(A_0)^2}{M_p^2}}. \quad (6)$$

After the symmetry breaking, the minima of the effective potential are determined using equation $V_{\text{eff.},A_0} = 0$, which leads to

$$A_0^{\text{min}} = \pm \sqrt{\frac{M_p^2}{\beta} \ln \left[\frac{m_A^2 M_p^2}{2\beta\rho} \right]}. \quad (7)$$

Furthermore, the quantity

$$m_{\text{eff.}}^2 = V_{\text{eff.},A_0 A_0}(A_0^{\text{min}}) = 2m_A^2 \ln \left[\frac{m_A^2 M_p^2}{2\beta\rho} \right] \quad (8)$$

gives the effective mass of the vector field outside the object. Note that the vector field's effective mass depends explicitly on the ambient matter density ρ .

The effective potential (6) exhibits a symmetry-breaking mechanism by lowering the density. At very high densities, the effective potential has only one critical point located at the origin so that the vector field has a vanishing vacuum expectation value. The mass of the fluctuations around $A_0 \rightarrow 0$ is $m_{\text{eff.}}^2 \simeq 2\beta\rho/M_p^2$. On the other hand, when the density is low enough, the field starts to run away from the tachyonic critical point at the origin. In the new vacuum, corresponding to the effective potential after the symmetry breaking, we have two minima with the effective mass given by Eq.(8).

We are interested in the vector field profile around static and spherically symmetric astrophysical sources, such as the Sun. The field equation in spherical coordinates reduces to

$$\frac{d^2 A_0}{dr^2} + \frac{2}{r} \frac{dA_0}{dr} = - \left[m_A^2 - \frac{2\beta\rho}{M_p^2} e^{\beta(A_0)^2/M_p^2} \right] A_0. \quad (9)$$

For outside the body with density ρ_0 , we assume that we are in the symmetry-breaking phase to expand the equations to linearize them around the corresponding minimum point. In such a case, the above equation for the perturbation of the field with respect to its background value A_0^{min} and for inside and outside is given by

$$\frac{d^2 \delta A_0}{dR^2} + \frac{2}{R} \frac{d\delta A_0}{dR} = m_{\text{in}}^2 R_\odot^2 (A_0^{\text{min}} + \delta A_0), \quad (R < 1) \quad (10)$$

and

$$\frac{d^2 \delta A_0}{dR^2} + \frac{2}{R} \frac{d\delta A_0}{dR} = m_{\text{out}}^2 R_\odot^2 \delta A_0, \quad (R > 1) \quad (11)$$

where $\delta A_0 \equiv A_0 - A_0^{\text{min}}$, and m_{in} and m_{out} are the vector field's effective masses inside and outside the Sun. We have written relations in terms of the dimensionless fractional radius $R \equiv r/R_\odot$.

The obtained equation looks similar to those in [37,38], so we can proceed similarly to obtain the solutions inside and outside the object of slowly varying density ρ_\odot and radius R_\odot . We use the following boundary conditions

$$\begin{aligned} \frac{d\delta A_0}{dr} &\longrightarrow 0 \quad \text{at } r \rightarrow 0 \\ \delta A_0 &\longrightarrow 0 \quad \text{at } r \rightarrow \infty \end{aligned} \quad (12)$$

to obtain a regular solution to these equations in a spherically symmetric static background. The analytical solution to the vector field equations (10) and (11) is

$$\delta A_0^{\text{in}}(R) = -A_0^{\text{min}} + \frac{C_1}{m_{\text{in}} R_\odot R} \sinh [m_{\text{in}} R_\odot R], \quad (R < 1) \quad (13)$$

and

$$\delta A_0^{\text{out}}(R) = C_2 \frac{1}{R} e^{-m_{\text{out}} R_{\odot} R}. \quad (R > 1) \quad (14)$$

To specify the constants A and B , we should use the continuity of the field and its first derivative at the $R = 1$, which leads us to

$$\begin{aligned} C_1 &= \frac{A_0^{\text{min}} m_{\text{in}} (1 + m_{\text{out}} R_{\odot})}{m_{\text{out}} \sinh(m_{\text{in}} R_{\odot}) + m_{\text{in}} \cosh(m_{\text{in}} R_{\odot})}, \\ C_2 &= -e^{m_{\text{out}} R_{\odot}} \frac{A_0^{\text{min}}}{R_{\odot}} \frac{m_{\text{in}} R_{\odot} \cosh(m_{\text{in}} R_{\odot}) - \sinh(m_{\text{in}} R_{\odot})}{m_{\text{in}} \cosh(m_{\text{in}} R_{\odot}) + m_{\text{out}} \sinh(m_{\text{in}} R_{\odot})}. \end{aligned} \quad (15)$$

In Figure 1, we show the profile corresponding to the above solution, where we see the analog of the thin-shell effect and how the field profile goes to zero very rapidly inside the object.

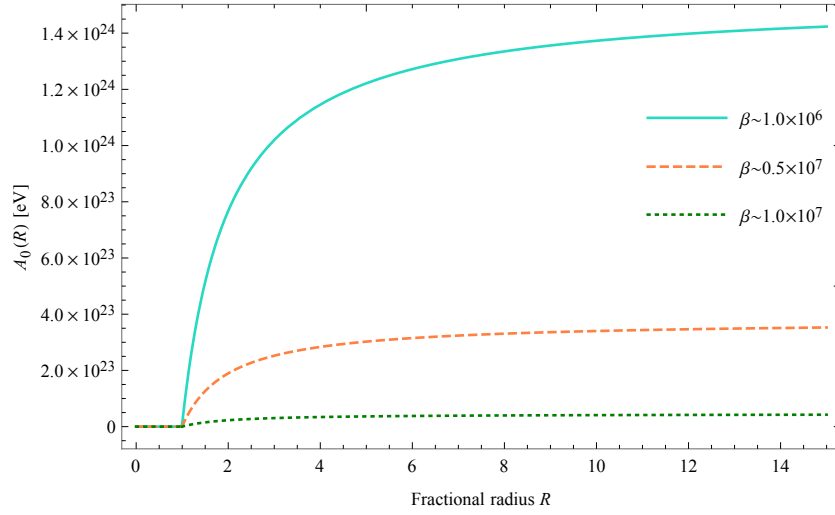


Figure 1: Shown is the vector field plot with respect to the fractional radius. We have tuned different values of β for the coupling strengths between vector and matter fields.

3 NSI with a light vector boson

As mentioned in section 2, the vector field's behavior is determined by matter density in the environment. Hence, this density implicitly affects the neutrino oscillation. The neutrino sector in the Lagrangian is given by:

$$\tilde{S}_\nu = \int d^4x \sqrt{-\tilde{g}} \bar{\psi}(x) \left[i\tilde{\gamma}^\mu \tilde{D}_\mu - m - g\tilde{\gamma}^\mu A_\mu \right] \psi(x), \quad (16)$$

where m is the neutrino mass, and g is the coupling coefficient between neutrinos and the vector component. The gamma matrices and also the covariant derivative [4] are

$$\tilde{\gamma}^\mu = B^{-1} \gamma^\mu, \quad (17)$$

and

$$\tilde{\gamma}^\mu \tilde{D}_\mu = B^{-1} \gamma^\mu D_\mu + \frac{3}{2} B^{-2} B_{,\mu} \gamma^\mu. \quad (18)$$

Varying the action (16) with respect to $\bar{\psi}$, the corresponding Dirac equation for neutrinos is obtained by

$$\gamma^\mu \left[p_\mu + gA_\mu - \frac{3}{2} i \partial_\mu \ln B \right] \psi + (mB)\psi = 0. \quad (19)$$

The effects of the conformal coupling can be interpreted as neutrino-vector interactions, specified by the terms including B . According to this equation, the effect of A_μ on neutrino propagation can be described as a correction either in the neutrino's mass

$$m \longrightarrow m' \equiv mB, \quad (20)$$

or four-momentum

$$p_\mu \longrightarrow p'_\mu \equiv p_\mu + gA_\mu - \frac{3}{2}i\partial_\mu \ln B. \quad (21)$$

The timelike component of Eq.(21) shows the shift in the neutrino energy, i.e.,

$$E = p_0 \longrightarrow E' = E + gA_0, \quad (22)$$

and also the momentum's spacelike component, i.e.,

$$p_z \longrightarrow p'_z = p_z - \frac{3}{2}i\partial_z \ln B \quad (23)$$

contains the damping signatures caused by the vector-matter field coupling $B(A^2)$. The quantity $V_W \equiv gA_0$ is the Wolfenstein potential coming from vector-neutrino NSI. So we encounter a Wolfenstein-like potential induced by a light vector mediator, which follows a spontaneous symmetry-breaking screening mechanism (see section 2).

Assuming $m' \ll E'$, the neutrino wavefunction is therefore given by

$$\begin{aligned} \psi_i(t, z) &= \sqrt{\mathcal{D}(z)} e^{i\varphi_i(t, z)} \psi_i(t_0, z_0) \\ &\equiv \mathcal{F}_i(t, z) \psi_i(t_0, z_0), \end{aligned} \quad (24)$$

where the oscillation phase is written as

$$\varphi_i(t, z) = E(t - t_0) - (E + gA_0)(z - z_0) + \int_{z_0}^z \frac{m_i^2 B^2}{2(E + gA_0)} dz. \quad (25)$$

The quantity

$$\mathcal{D}(z) \equiv [B(z)B^{-1}(z_0)]^{-3} \quad (26)$$

is defined to be a damping/enhancing factor that changes the neutrino flavor transition probabilities. These damping signatures are minor perturbations to the neutrino oscillations in a nearly constant matter density. Since the field value is tiny inside the object, as shown in Fig.1, the damping effects are smooth inside the Sun. Note that the direction of solar neutrinos propagating to the Earth is assumed to be the z -axis. In other words, we are working at the $\theta_{\text{polar}} = 0$ plane, i.e., $z = r$.

The oscillation phase is explicitly given by

$$\Phi_{ij}(r) = \int_{r_0}^r \Delta m_{ij}^2 \left[\frac{B^2(r)}{2(E + gA_0(r))} \right] dr, \quad (27)$$

where we have assumed that the vector-neutrino couplings g are all the same, and $\Delta m_{ij}^2 := m_i^2 - m_j^2$. Note that the above oscillation phase difference can be obtained by replacing $E \rightarrow E + gA_0(r)$ in the usual phase $\int p_\mu dx^\mu$ [37]. The energy-momentum relation is given by $[E + gA_0(r)]^2 = p_z^2 + B^2(r)m^2$ in this case.

Based on the wavefunction (24), the state of neutrinos can be written as [4]

$$|\nu(r, t)\rangle_\alpha = \sum_{i, \beta} \mathcal{F}_i(r, t) \psi_i(r_0, t_0) U_{\alpha i}^* U_{\beta i} |\nu_\beta\rangle, \quad (28)$$

where $U_{\alpha i}$'s are the elements of the unitary mixing matrix. Assume that the flavor of neutrinos produced at the source is ν_α ; then, the probability of transition $\alpha \rightarrow \beta$ is given by

$$P_{\alpha\beta} = \frac{\left| \langle \nu_\beta | \nu(r, t) \rangle_\alpha \right|^2}{\left| \langle \nu_\alpha | \nu(r_0, t_0) \rangle_\alpha \right|^2} = \sum_{i, j} \mathcal{F}_i(r, t) \mathcal{F}_j^*(r, t) U_{\alpha i}^* U_{\beta i} U_{\alpha j} U_{\beta j}^*. \quad (29)$$

Defining $c_{ij} \equiv \cos \theta_{ij}$ and $s_{ij} \equiv \sin \theta_{ij}$, the electron-neutrino survival probability is given by

$$P_{ee} = \mathcal{D}(r) [c_{12}^4 c_{13}^4 + s_{12}^4 c_{13}^4 + s_{13}^4 + 2c_{12}^2 s_{12}^2 c_{13}^4 \cos(\Phi_{12}(r)) + 2c_{12}^2 c_{13}^2 s_{13}^2 \cos(\Phi_{13}(r)) + 2s_{12}^2 c_{13}^2 s_{13}^2 \cos(\Phi_{23}(r))]. \quad (30)$$

By substituting from Eq.(29), we have the following transition probabilities for the two-flavor case:

$$P_{ee} = \mathcal{D}(r) \left[1 - \sin^2(2\theta) \sin^2 \left(\frac{\Phi_{12}(r)}{2} \right) \right], \quad (31)$$

and

$$P_{e\mu} = \mathcal{D}(r) \sin^2(2\theta) \sin^2 \left(\frac{\Phi_{12}(r)}{2} \right). \quad (32)$$

Although more tedious, the probabilities for the three-flavor may be derived in the same way. We can compare these relations with the KamLAND electron-antineutrino results [3,35] to constrain the parameters of this scenario.

4 MSW effect and vector-neutrino NSI

The MSW flavor transformation is an explicit formulation of the Standard Model and neutrino transition inside matter. Any non-standard interaction with matter that influences neutrino states can change the ν_e survival probability prediction. We include all interactions in the Hamiltonian to see how the coupling to vector boson affects the neutrino flavor change. For the 2ν case, we then have

$$\mathcal{H} = \frac{1}{4E} \left[\Delta \hat{m}^2 \begin{pmatrix} -\cos 2\theta & \sin 2\theta \\ \sin 2\theta & \cos 2\theta \end{pmatrix} + \mathcal{A} \begin{pmatrix} 1 & 0 \\ 0 & -1 \end{pmatrix} \right], \quad (33)$$

where $\Delta \hat{m}^2(r) \equiv \left[B^2(r) / \left(1 + \frac{gA_0(r)}{E} \right) \right] \Delta m^2$, and $\mathcal{A} = 2\sqrt{2}G_F n_e E$ is from the effective matter potential describing the standard interaction of electron-neutrinos with left-handed electrons through the exchange of W bosons. Using this Hamiltonian in the Schrödinger-like equation

$$i \frac{d}{dL} \begin{pmatrix} \nu_e \\ \nu_\mu \end{pmatrix} = \mathcal{H} \begin{pmatrix} \nu_e \\ \nu_\mu \end{pmatrix} \quad (34)$$

for ultra-relativistic neutrinos propagating the distance L , one can easily derive the two-flavor neutrino survival probability $\langle P_{ee} \rangle$. Henceforth, the critical point is to diagonalize the effective Hamiltonian Eq.(33) and to derive the explicit expressions for the effective oscillation parameters. The solar neutrino parameters of this model correspond to the LMA-MSW solution. These are related to the vacuum mixing parameters $(\theta, \Delta m^2)$ by

$$\sin 2\theta_{\mathcal{M}} = \frac{\Delta \hat{m}^2 \sin 2\theta}{\Delta m_{\mathcal{M}}^2}, \quad (35)$$

and

$$\Delta m_{\mathcal{M}}^2 = \sqrt{[\Delta \hat{m}^2 \cos 2\theta - \mathcal{A}]^2 + [\Delta \hat{m}^2 \sin 2\theta]^2}. \quad (36)$$

In the matter regime, the damping contribution can be derived in the same way as the vacuum case, starting from the following neutrino state for neutrinos produced at the Sun's core and detected on the Earth:

$$|\nu(t, r)\rangle_\alpha = \sum_{i, \beta} \mathcal{F}_i(t, r) \psi_i(t_0, r_0) U_{\beta i}(\theta, r) U_{\alpha i}^*(\theta_M, r_0) |\nu_\beta\rangle. \quad (37)$$

Here $U_{\alpha i}(\theta_M, r_0)$ and $U_{\beta i}(\theta, r)$ are the mixing matrix elements in the matter at the production point and in the vacuum at the detection point. Then,

$$\langle P_{ee} \rangle = \mathcal{D}(r) [\cos^2 \theta \cos^2 \theta_M + \sin^2 \theta \sin^2 \theta_M], \quad (38)$$

and

$$\langle P_{e\mu} \rangle = \mathcal{D}(r) [\sin^2 \theta \cos^2 \theta_M + \cos^2 \theta \sin^2 \theta_M] \quad (39)$$

give the damped probabilities on the Earth, where θ_M is the effective mixing angle inside the Sun. Due to the considerable distance between the Sun and Earth, we could take the averaged oscillation probabilities. We have defined a general damping signature (26) to be an effect that alters the neutrino flavor conversion probabilities to the above forms. So, the total probability

$$\langle P_{\text{tot.}} \rangle = \langle P_{ee} \rangle + \langle P_{e\mu} \rangle \leq 1, \quad (40)$$

may not be conserved in such cases. The equality holds if and only if the \mathcal{D} -factor is set to zero. Expressed in terms of the damping factor, the quantity

$$\delta P_{e \rightarrow A} = 1 - \mathcal{D}(r) \quad (41)$$

determines the deviation of the total probability from unity. The most convincing explanation of transitions among various neutrino flavor eigenstates is probably the neutrino oscillation; however, all the probabilities above also suffer explicitly from damping treatment indicating an extra deficiency in the neutrino flux on Earth. This deficiency can be considered an outcome of neutrinos decay to vector bosons. Therefore, we collect these non-standard interactions in a framework together with neutrino oscillations, which are assumed as the leading order effect and can be constrained by current [39] and future experiments [40, 41].

5 Results, discussions and conclusion

We studied neutrino interaction with a light vector boson by considering an additional conformal coupling that allows a screening mechanism based on the \mathbb{Z}_2 symmetry breaking. Neutrino propagation inside and outside a spherical object like the Sun can be affected via this NSI, such that both mass and energy terms of the neutrinos are modified, contrary to the Refs. [8] and [10].

In section 2, a vector screening model, consisting of a massive vector field that is conformally coupled to matter, was introduced. Such a screening mechanism here occurs due to a spontaneous symmetry breaking. We obtained the vector field solution by expanding the field around its background value, i.e., $A_0 = A_0^{\text{min}} + \delta A_0$.

The solution to the Dirac equation was derived in section 3 and employed to study the neutrino flavors oscillation.

The NSI modifies the solar neutrino transition probabilities via the MSW effect as the neutrinos propagate through dense solar matter. We obtained the effective Hamiltonian induced by both matter electrons and vector components in section 4. From the damping factor \mathcal{D} , we concluded that the sum of various probabilities is assumed not equals to unity, meaning there is a decay possibility along neutrinos' journey.

In the following, we illustrate numerically some of the effects of NSI on neutrino flavor conversion. For this purpose, we employ the numerical values $m_A \gtrsim 10^{-27} \text{eV}$ for the vector field's mass [26], and $\tan^2 \theta_{12} = 0.41$, $\sin^2 2\theta_{23} \simeq 0.99$, $\sin^2 2\theta_{13} \simeq 0.09$,

$$\Delta m_{21}^2 = 7.4 \times 10^{-5} \text{eV}^2,$$

and

$$|\Delta m_{23}^2| = 2.5 \times 10^{-3} \text{eV}^2$$

for neutrino's mass and mixing parameters [42]. We observe the effect of the NSI on the solar electron-neutrino survival probability in figures 2 and 3. A comparison with Borexino [34] and SNO+SK [35] observational data has also been given in both plots.

Fig.2 illustrates the probability $\langle P_{ee}(E_\nu) \rangle$ for some different choices of β , caused by the modified MSW effect. As can be seen, the theoretically predicted shift of $\langle P_{ee}(E_\nu) \rangle$ is mainly within the error bars

of the experimentally determined values of Borexino. For weaker couplings β , the damping signatures more appear in the survival probability, such that $\langle P_{ee}(E_\nu) \rangle$ drops down to ~ 0.33 for $\beta \sim 0.6 \times 10^7$.

We note that the optimal flavor mixing occurs whenever $\sin^2 2\theta_{\mathcal{M}} = 1$, resulting in the resonance energy, i.e.,

$$E_{\text{res.}}^\odot = \frac{\Delta m^2 B^2(r_{\text{res.}}) \cos 2\theta}{2\sqrt{2}G_F n_e(r_{\text{res.}})} - gA_0(r_{\text{res.}}). \quad (42)$$

Since the resonance energy is explicitly dependent on the vector-matter coupling strengths β and vector-neutrino coupling coefficient g , this is expected that there would be a shift in the resonance energy for various coupling strengths. From this figure, it is evident that the resonance energy decreases when we increase the coupling β .

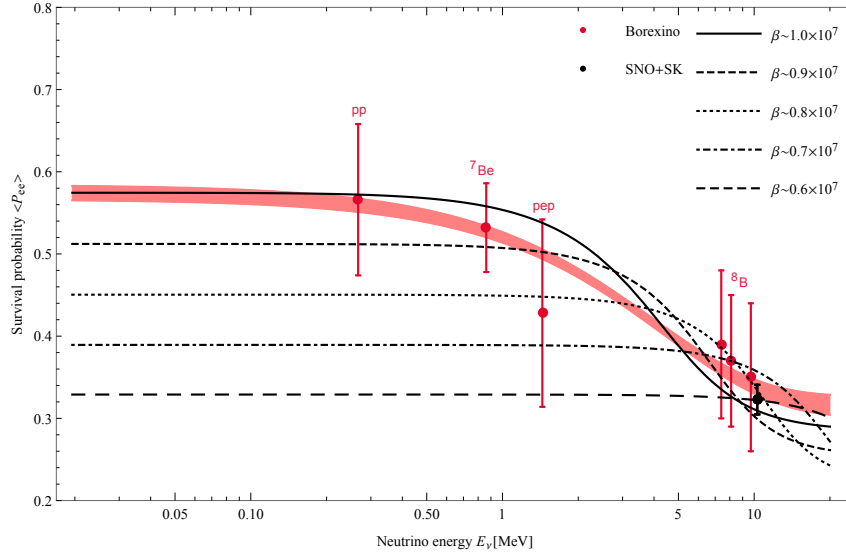


Figure 2: The survival probability as a function of energy with various LMA-MSW + NSI cases. The pink band shows the standard effects. We have assumed that $g \sim 5 \times 10^{-8}$.

We also show the effect of the vector NSI on the solar neutrino survival probability in Fig.3 for various ν -vector couplings g . The presence of the non-zero coupling parameter g will also shift the resonance energy. Larger couplings result in higher values of $E_{\text{res.}}^\odot$. Furthermore, for $g \gtrsim 10^{-5}$, the probability $\langle P_{ee} \rangle$ tends to Vacuum-LMA scenario that assumes all solar neutrinos oscillate in the vacuum regime.

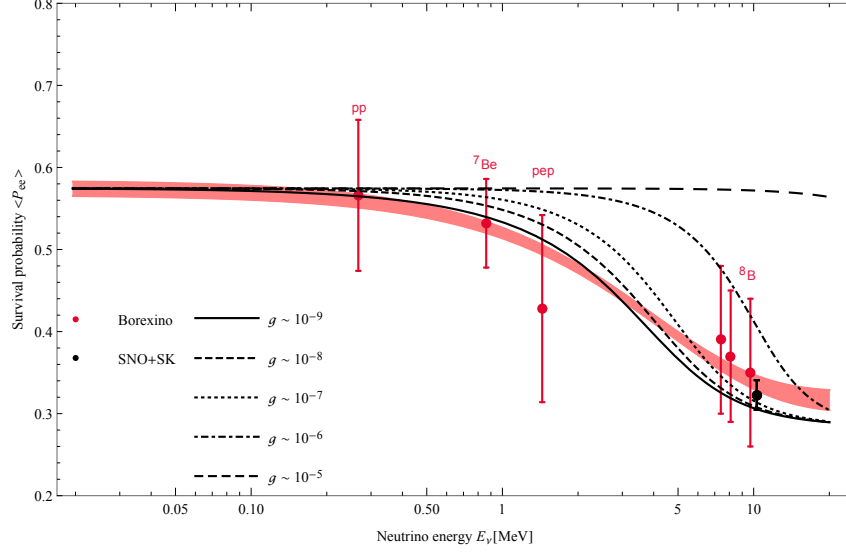


Figure 3: The solar neutrino survival probabilities with the vector NSI, together with the Borexino measurement [34] of the pp, ${}^7\text{Be}$, pep, and ${}^8\text{B}$ fluxes. The black point also represents the SNO + SK ${}^8\text{B}$ data [35]. This figure is plotted for $\beta \sim 1.0 \times 10^7$.

The NSI might provide a change in different transition probabilities. As shown in Fig. 4, the $\beta \sim 1.0 \times 10^7$ and $g \sim 5 \times 10^{-8}$ can modify the flavor conversion behaviors, especially on the total number density of neutrinos. The loss probability $\delta P_{e \rightarrow A}$ is shown in this figure. From Eq.(37), it is apparent that the loss probability declines for increasing β . As shown in the plot, $\delta P_{e \rightarrow A}$ goes to zero for $E_\nu \gtrsim 10\text{MeV}$.

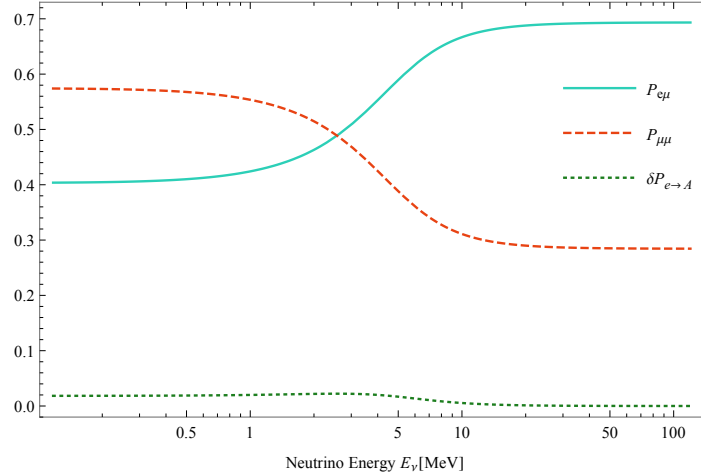


Figure 4: The curves illustrate probabilities $P_{e\mu}$, $P_{\mu\mu}$ and $\delta P_{e \rightarrow A}$, for $\beta \sim 1.0 \times 10^7$ and $g \sim 10^{-8}$.

In Fig. 5, we show the change of $\sin^2 2\theta_M$ in terms of neutrino energy, taking various coupling strengths β . The solid, dashed, and dotted curves correspond to the $\beta = 1.0 \times 10^7$, 0.8×10^7 , 0.6×10^7 , respectively. At low energies, $\sin^2 2\theta_M \rightarrow 1$ shows the standard (maximal) mixing at the peaks. As the neutrino energy increases, the mixing inside matter goes to zero. So, $\sin^2 2\theta_M$ becomes negligible, and thus the transition probability becomes low at this point.

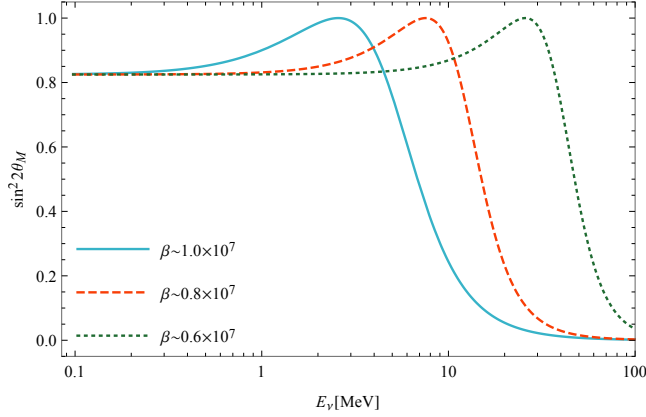


Figure 5: $\sin^2 2\theta_M$ as a function of neutrino energy E_ν . It is assumed that $g \sim 5 \times 10^{-8}$.

References

- [1] Y. Fukuda *et al.* [Super-Kamiokande], Phys. Rev. Lett. **81**, 1562-1567 (1998) [arXiv:hep-ex/9807003 [hep-ex]].
- [2] Q. R. Ahmad *et al.* [SNO], Phys. Rev. Lett. **89**, 011301 (2002) [arXiv:nucl-ex/0204008 [nucl-ex]].
- [3] A. Gando *et al.* [KamLAND], Phys. Rev. D **88**, no.3, 033001 (2013) [arXiv:1303.4667 [hep-ex]].
- [4] H. Mohseni Sadjadi and H. Y. Ahmadabadi, Phys. Rev. D **103**, no.6, 065012 (2021) [arXiv:2012.03633 [hep-ph]].
- [5] H. Y. Ahmadabadi and H. M. Sadjadi, “Non-standard neutrino interaction induced by conformal coupling,” [arXiv:2201.02927 [hep-ph]].
- [6] O. G. Miranda and H. Nunokawa, New J. Phys. **17**, no.9, 095002 (2015) [arXiv:1505.06254 [hep-ph]].
- [7] P. S. Bhupal Dev, K. S. Babu, P. B. Denton, P. A. N. Machado, C. A. Argüelles, J. L. Barrow, S. S. Chatterjee, M. C. Chen, A. de Gouvêa and B. Dutta, *et al.* SciPost Phys. Proc. **2**, 001 (2019) [arXiv:1907.00991 [hep-ph]].
- [8] S. F. Ge and S. J. Parke, Phys. Rev. Lett. **122**, no.21, 211801 (2019) [arXiv:1812.08376 [hep-ph]].
- [9] L. Wolfenstein, Phys. Rev. D **20**, 2634 (1979).
- [10] A. Y. Smirnov and X. J. Xu, JHEP **12**, 046 (2019) [arXiv:1909.07505 [hep-ph]].
- [11] L. Amendola, M. Baldi and C. Wetterich, Phys. Rev. D **78**, 023015 (2008) [arXiv:0706.3064 [astro-ph]].
- [12] A.W. Brookfield, C. van de Bruck, D.F. Mota, D. Tocchini-Valentini, Phys. Rev. Lett. **96**, 061301 (2006) [arXiv:0503349 [astro-ph]].
- [13] J. G. Salazar-Arias and A. Pérez-Lorenzana, Phys. Rev. D **101**, no.8, 083526 (2020) [arXiv:1907.00131 [hep-ph]].
- [14] S. Mandal, G. Y. Chitov, O. Avsajanishvili, B. Singha and T. Kahniashvili, JCAP **05**, 018 (2021) [arXiv:1911.06099 [hep-ph]].
- [15] M. Carrillo González, Q. Liang, J. Sakstein and M. Trodden, JCAP **04**, 063 (2021) [arXiv:2011.09895 [astro-ph.CO]].
- [16] A. R. Khalifeh and R. Jimenez, Phys. Dark Univ. **34**, 100897 (2021) [arXiv:2105.07973 [astro-ph.CO]].

- [17] J. Khoury and A. Weltman, Phys. Rev. Lett. **93**, 171104 (2004) [arXiv:astro-ph/0309300 [astro-ph]].
- [18] J. Khoury and A. Weltman, Phys. Rev. D **69**, 044026 (2004) [arXiv:astro-ph/0309411 [astro-ph]].
- [19] T. P. Waterhouse, “An Introduction to Chameleon Gravity,” [arXiv:astro-ph/0611816 [astro-ph]].
- [20] S. Tsujikawa, T. Tamaki and R. Tavakol, JCAP **05**, 020 (2009) [arXiv:0901.3226 [gr-qc]].
- [21] K. Hinterbichler, J. Khoury, A. Levy and A. Matas, Phys. Rev. D **84**, 103521 (2011) [arXiv:1107.2112 [astro-ph.CO]].
- [22] H. Mohseni Sadjadi, M. Honardoost and H. R. Sepangi, Phys. Dark Univ. **14**, 40-47 (2016) [arXiv:1504.05678 [gr-qc]].
- [23] H. Mohseni Sadjadi, JCAP **01**, 031 (2017) [arXiv:1609.04292 [gr-qc]].
- [24] M. Honardoost, D. F. Mota and H. R. Sepangi, JCAP **11**, 018 (2017) [arXiv:1704.02572 [gr-qc]].
- [25] H. Mohseni Sadjadi and V. Anari, arXiv:2205.15693 [gr-qc]
- [26] J. Beltran Jimenez, A. L. Delvas Froes and D. F. Mota, Phys. Lett. B **725**, 212-217 (2013) [arXiv:1212.1923 [astro-ph.CO]].
- [27] J. Park, T. Hoon Lee, Phys. Rev. D **101**, 123528 (2020) [arXiv:1908.04630 [gr-qc]].
- [28] H. Mohseni Sadjadi and V. Anari, Phys. Rev. D **95**, no.12, 123521 (2017) [arXiv:1702.04244 [gr-qc]].
- [29] H. M. Sadjadi and V. Anari, JCAP **10**, 036 (2018) [arXiv:1808.01903 [gr-qc]].
- [30] M. Sami, S. Myrzakul and M. Al Ajmi, Phys. Dark Univ. **30**, 100675 (2020) [arXiv:1912.12026 [gr-qc]].
- [31] L. Mastrototaro and G. Lambiase, Phys. Rev. D **104**, 024021 (2021) [arXiv:2106.07665[gr-qc]].
- [32] P. Sadeghi, F. Hammad, A. Landry, T. Martel, Gen. Relativ. Gravit. **53**, 98 (2021) [arXiv:2111.01441 [gr-qc]].
- [33] F. Hammad, P. Sadeghi and N. Fleury [arXiv:2209.03899 [hep-ph]].
- [34] M. Agostini *et al.* [BOREXINO], Nature **562**, no.7728, 505 (2018).
- [35] P. A. Zyla *et al.* [Particle Data Group], PTEP **2020**, 083C01 (2020).
- [36] J. A. R. Cembranos, C. Hallabrin, A. L. Maroto and S. J. N. Jareno, Phys. Rev. D **86**, 021301 (2012) [arXiv:1203.6221 [astro-ph.CO]].
- [37] H. Y. Ahmadabadi and H. Mohseni Sadjadi, Phys. Dark Univ. **37**, 101067 (2022) [arXiv:2111.03054 [hep-ph]].
- [38] H. Mohseni Sadjadi and A. P. Khosravi, JCAP **04**, 008 (2018) [arXiv:1711.06607 [hep-ph]].
- [39] B. Aharmim *et al.* [SNO], Phys. Rev. D **99**, no.3, 032013 (2019) [arXiv:1812.01088 [hep-ex]].
- [40] R. Acciarri *et al.* [DUNE], [arXiv:1512.06148 [physics.ins-det]].
- [41] F. An *et al.* [JUNO], J. Phys. G **43**, no.3, 030401 (2016) [arXiv:1507.05613 [physics.ins-det]].
- [42] I. Esteban, M. C. Gonzalez-Garcia, M. Maltoni, T. Schwetz and A. Zhou, JHEP **09**, 178 (2020) [arXiv:2007.14792 [hep-ph]]; see also www.nu-fit.org.